

The DoPHOT Two-Dimensional Photometry Program

Mario Mateo

The Observatories of the Carnegie Institution of Washington
Pasadena, CA 91101, USA

Paul L. Schechter

Massachusetts Institute of Technology, Department of Physics
Cambridge, MA 02139, USA

Abstract

We describe the two-dimensional photometry reduction program **DoPHOT** which is designed to reduce images automatically. We describe how the program iteratively finds and classifies objects, updates the PSF, and fits the current best-estimate of the PSF to all stellar images. The shortcomings and advantages of the approach used by **DoPHOT** are discussed in some detail. Some of the qualitative and quantitative tests that we have performed using the ESO test images as well as other images at our disposal are also described. The flexibility of the code is demonstrated by the wide variety of scientific problems that are being successfully addressed with the help of **DoPHOT**. Finally, we present future plans for changes and improvements of the code.

1 Introduction

Using modern two-dimensional electronic detectors, an observer can readily generate 10^8 pixels of linear, photometric data in a single night. These observations may consist of guided CCD exposures of the central regions of globular clusters, or CCD drift scans of low Galactic latitude fields, or deep CCD exposures of distant galaxy clusters, and could contain useful photometry of up to 10^5 objects from hundreds of individual frames. The **DoPHOT** two-dimensional photometry reduction program was developed by one of us (PS) to reduce large quantities of high-quality, linear digital data such as these quickly, and in a nearly completely automated manner. **DoPHOT** was originally designed to reduce CCD drift scans of stars at the south Galactic pole, but the code is quite flexible, and it has now been used successfully to reduce a wide variety of CCD data including not only drift scans but more traditional guided exposures as well.

In this contribution, we describe how **DoPHOT** works, and emphasize some of the features that distinguish it from other photometry programs. We also briefly describe some of the quantitative and qualitative tests that have been performed to assess the performance of **DoPHOT**, including results based on the analysis of the ESO test images distributed for this workshop. As a supplement to this paper and to facilitate future comparisons, a VAX backup tape will be available at ESO headquarters containing the detailed photometric results of our **DoPHOT** reduction of the ESO test images. We conclude with a summary of the sorts of scientific problems that are currently being addressed with the help of **DoPHOT**, and a discussion of future plans for improvement and distribution of the code.

Proceedings of 1st ESO/ST-ECF Data Analysis Workshop, April 17-19, 1989

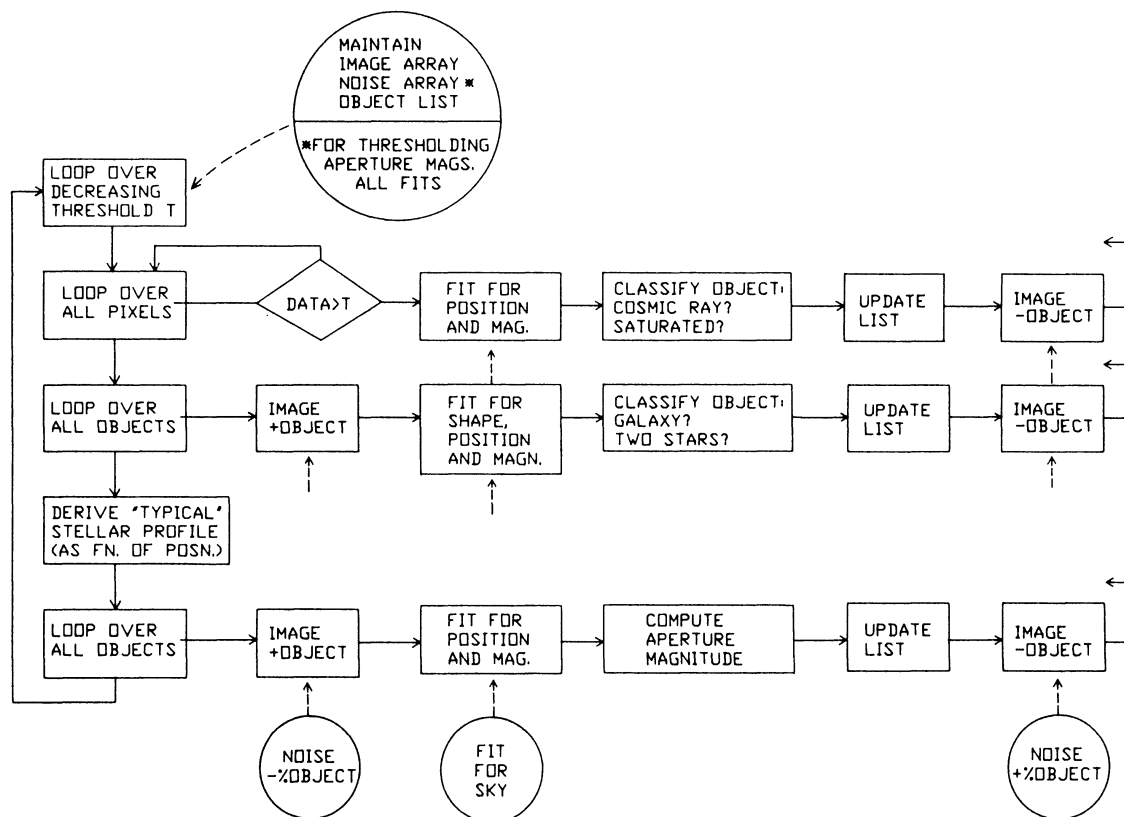


Figure 1: A flowchart summarizing the operation of DoPHOT.

2 A DoPHOT Primer: Theory and Practice

DoPHOT was inspired by R. Lupton's **WOLF** stellar photometry program [2], and there are a number of conceptual similarities between the codes. However, the programs are implemented differently, and whereas DoPHOT was designed from its inception to run in an automatic mode, a significant amount of human time was required by early versions of **WOLF**.

DoPHOT assumes that the input data consist of an array of linear intensities. In this paper, we further assume that this array is a guided CCD image that has been appropriately processed to correct for instrumental effects (e.g., bias subtraction, flat-field correction, and/or bad pixel and cosmic ray removal). There is no fundamental limit to the size of picture that DoPHOT can handle, but in practice such limits are imposed by the available virtual memory and disk storage on the user's machine. DoPHOT is written in FORTRAN and currently runs on VAXes running VMS and Berkeley 4.3 Unix operating systems. The code uses some matrix inversion routines from *Numerical Recipes* [4] which are publicly available.

Figure 1 is a flowchart illustrating the basic steps in the reduction of a digital image by DoPHOT. The purpose of this section is to describe these steps in some detail.

2.1 DoPHOT's Arrays

At startup, DoPHOT generates two arrays which are referred to as the cleaned array and the noise array. Both arrays have the same dimensions as the original picture array, and they are frequently used by the program. The cleaned array is an updated record of the residuals of the fits to all objects that DoPHOT finds and measures, and initially it is an exact duplicate of the original picture. All of the photometric measurements performed by DoPHOT are carried out on the cleaned array. The noise array contains the variance of each pixel in the picture array. Initially, it is set equal to the square of the readout noise (which is specified by the user) plus the number of detected electrons (i.e., the variance of the Poisson noise). The manner in which DoPHOT uses these two important arrays is described below.

2.2 The Point-spread-function (PSF)

In its current form, DoPHOT assumes that the stellar PSF can be approximated by an analytic function with seven free parameters. The form of this function can be selected by the user depending on the application, and a number of different PSFs have been tested. The results reported in this paper were obtained using a two-dimensional, elliptical Gaussian PSF of the form,

$$I(x, y) = h \exp \left[-\frac{1}{2} \left(\frac{x^2}{\sigma_x^2} + 2\sigma_{xy}xy + \frac{y^2}{\sigma_y^2} \right) \right] + s, \quad (1)$$

where $x = (x' - x_0)$ and $y = (y' - y_0)$, where (x_0, y_0) is the nominal center of the PSF. In practice, the exponential function in equation 1 is approximated by

$$e^{-z} \approx \left(1 + z + \frac{1}{2}z^2 + \frac{1}{6}z^3 \right)^{-1}. \quad (2)$$

This expression has two practical advantages: it can be evaluated more quickly than an exponential function, and it is 'wingier' than a true Gaussian as most PSFs are observed to be. The seven free parameters in this function are: the shape parameters σ_x , σ_y , and σ_{xy} ; the image center, (x_0, y_0) ; the central intensity, h ; and the background intensity, s . DoPHOT's ultimate job is to determine the appropriate shape parameters for a given frame, and the centers, central intensities, and sky backgrounds for each object. At any given time, the program stores a set of average shape parameters which correspond to the shape parameters that best describe the single PSF for the entire frame. DoPHOT *can* handle cases where the average shape parameters are a function of location on the frame; this mode of operation has been used successfully to reduce scanning CCD data. When the program is started, the user supplies initial guesses for the average shape parameters by specifying the typical FWHM of stellar images on the frame. Thereafter, DoPHOT determines and updates the average shape parameters automatically.

There are two basic sorts of PSF fits that are performed by DoPHOT. First, for a given object the program can assume that the average shape parameters apply and only the central position, central intensity, and sky background are allowed to vary. We refer to such fits as 4-parameter fits. In contrast, a 7-parameter fit involves solving for all of the PSF parameters simultaneously. Note that for both 4- and 7-parameter fits, DoPHOT solves for the local sky value explicitly. Both sorts of fits are performed within rectangular subrasters extracted from the cleaned array and centered on an initial guess to the fitted object's position. Each pixel in the subraster is weighted by the inverse of the corresponding variance stored in the noise array. The fit subrasters's dimensions can be adjusted by the user.

2.3 Thresholds

Many tasks must be performed by DoPHOT in order to adequately reduce a CCD image. For example, the program must not only find and classify objects, but it must also generate the PSF for the picture, execute two-dimensional profile fits for each identified object, and assess the quality of these fits. Moreover, all of this must be done automatically. Rather than attempt to accomplish these tasks in a single pass through the data, DoPHOT loops through every pixel of the picture many times (this is represented by the leftmost loop in Figure 1). Each loop is governed by a number, known as the threshold, which corresponds to the minimum intensity an object must have (above local sky) in order for DoPHOT to attempt to identify and possibly measure that object during that loop. When a loop is completed, the threshold is lowered and the process is repeated until the lowest threshold is reached. At the beginning of the reduction of a frame, the user specifies the minimum and maximum thresholds, as well as the ratio of successive thresholds. For $T_{min} = 50$, $T_{max} = 15000$, and $\Delta T = 2$, DoPHOT would pass through the data nine times, and the uppermost threshold would be 12800.

To ensure that the thresholds are applied uniformly over the entire frame, DoPHOT attempts to account for any regular variations in the background. For example, a frame containing the center of a concentrated globular cluster (such as the ESO test images of 47 Tuc) clearly has a higher local sky value at the cluster center than further out (see Figure 2). If such background variations were ignored, DoPHOT could mistakenly identify and fit regions of locally enhanced backgrounds as clumps of individual stars. The program attempts to solve this problem by taking the sky values determined for individual stars located throughout the picture and fitting these values to an analytic function that approximates the unresolved background variations in the data. This background is used solely to determine future thresholds as a function of position across the frame – *not* to estimate the sky values for any stars. This procedure is illustrated schematically in Figure 2. A number of different analytic functions have been used to model the background for different frames and the user must select the most appropriate model for his particular data. In the case of the ESO test images of the center of 47 Tuc, we used a Hubble-law to model the background light from the unresolved, faint cluster stars.

2.4 Finding Objects and Initial Classification

At the start of any threshold loop, DoPHOT identifies all potential objects in the cleaned array with peak intensities which exceed the current threshold. The program then tries to decide if these potential objects are a) too faint to be fit, b) too bright to be fit, c) cosmic rays, or d) legitimate objects that can be classified and measured more carefully later. The subroutine in DoPHOT that controls these tasks is called ISEARCH and it is represented by the top line of the flowchart shown in Figure 1.

Assuming that DoPHOT has found the location of a pixel whose value exceeds the current threshold, the program asks the following question: At the position of the brightest pixel near this location, is the ratio of a ‘masked’ signal divided by a ‘masked’ noise larger than some parameter B ? The ‘mask’ referred to is a ‘normalized’ weighting function based on the adopted analytic PSF. An example of such a mask (and the one used in the reductions reported here) is equation 1 with $h = 1$, $s = 0$, and centered on the pixel in question. By using a PSF mask, DoPHOT optimizes its chances to find objects near their true centers. The default value for B is 4, although this can be changed by the user depending on his needs.

If DoPHOT finds an object in this way, it determines if it contains an excessive number of saturated pixels. If so, the program obliterates this region of the cleaned by flagging a region surrounding these pixels in the noise array. These obliterated regions will never be used in any subsequent PSF fits. The obliteration parameters are controlled by the user, and they should be tuned for the

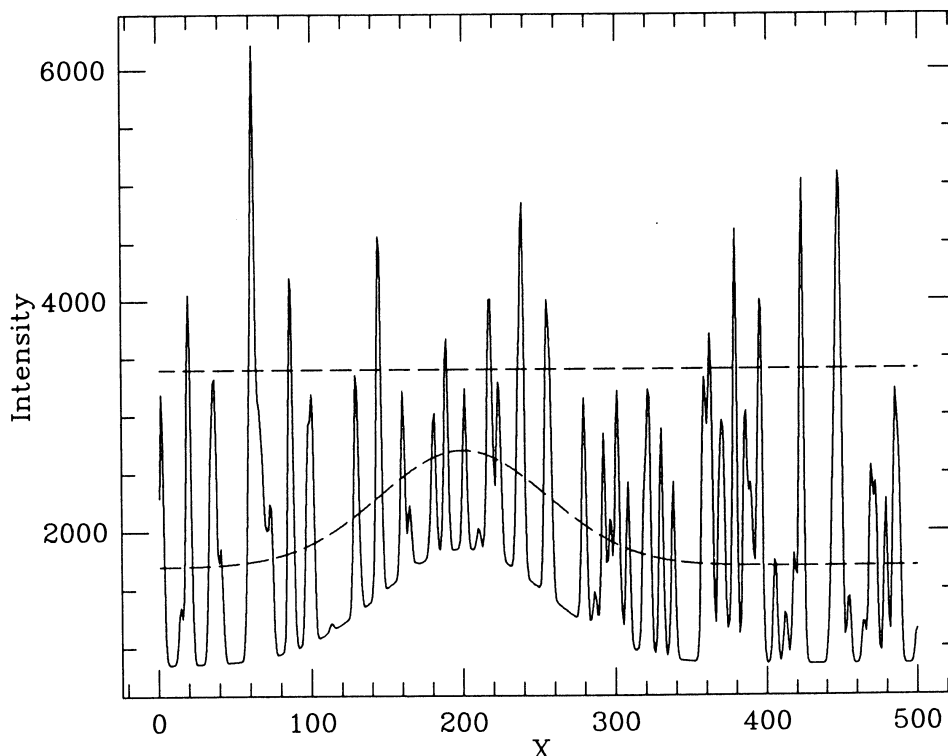


Figure 2: A schematic illustration of how DoPHOT sets its thresholds. The solid curve is a cut across a hypothetical cluster of stars. Many of the bright, resolved stars are clearly visible, but there is also an unresolved background from numerous faint cluster members. Assume that the top dashed line corresponds to the first threshold, and that DoPHOT successfully identifies and performs PSF fits to all stars whose central intensities exceed this threshold. The sky values of these fits are themselves then fit to a Hubble-law profile, and the next threshold is measured relative to this fit to the background light as shown by the lower dashed line. Note that the background fit is *not* used to estimate the actual sky values for any stars.

particular detector used. The premise behind this method of dealing with saturated pixels is that even unsaturated stars very near saturated objects probably cannot be measured accurately; thus it is best to ignore that part of the picture altogether. Another possibility is that the object found by DoPHOT is a single high pixel – for example a cosmic ray or a chip defect. If so, only that one pixel is obliterated. As with most photometry reduction routines, DoPHOT may confuse larger cosmic ray events as legitimate stars. These cases can still be distinguished later on, however, if there are other frames of the same field or by using the fact that such ‘stellar’ cosmic rays tend to have abnormally large formal errors compared the errors of true stars with similar central intensities.

If DoPHOT can find no good reason at this point to ignore or otherwise reject the newly found object, it performs a 4-parameter fit, stores the object’s location, and subtracts the best-fitting PSF from the cleaned array. At the same time, a fraction (specified by the user) of the square of the image profile is added to the noise array at the same location. This last step acknowledges that the actual PSF and the analytic PSF may not match precisely; the residuals of a subtracted star in the cleaned array primarily reflect this mismatch. Because all fits are weighted by the inverse of the variances stored in the noise array, this procedure forces DoPHOT to give smaller weight to pixels near previously subtracted images. When DoPHOT *adds* stars to the cleaned array, the variances are subtracted from the noise array in the same way.

2.5 Refining the PSF

The second major set of tasks that DoPHOT must accomplish during each threshold loop is represented by the second horizontal line in Figure 1. These tasks are controlled by the subroutine SHAPE. This routine a) performs a 7-parameter PSF fit to each of these objects, and b) determines which ones are single stars, double stars, or galaxies. SHAPE is a particularly crucial component of DoPHOT because it is the only place where 7-parameter fits are performed and because the determination of the average PSF shape parameters depend entirely on such fits.

The SHAPE routine begins by looping through *all* the objects found by earlier passes through ISEARCH. Cosmic rays, obliterated stars, and previous non-converging stars are skipped. One-by-one, the remaining objects are added to the cleaned array using their shape parameters and the analytic PSF (equation 1 in the present case) and the noise array is updated accordingly. If DoPHOT had found every object on the frame prior to this, and if the PSF and its parameters were perfectly determined, then the cleaned array would contain *just this one star*. In general, not all objects are detected (even after the lowest threshold loop) and the PSF is never perfect. Nevertheless the added star is now more isolated than it had been on the original frame because some, and perhaps most, of its neighbors have been subtracted. A 7-parameter fit is then performed on the added star. Three things can happen at this point: 1) the fit does not converge, 2) the fit converges, but the shape parameters are considerably larger than the average shape parameters, or 3) the fit converges, and the shape parameters are consistent with the average shape parameters. Extremely narrow objects are rarely found at this stage because of the earlier removal of cosmic rays by ISEARCH. In case 1, the object is flagged as a non-converger and it is skipped by SHAPE. In case 2, the object is treated as either a galaxy or a double star. DoPHOT defines a galaxy as an object in which the shape parameters are considerably larger than the average shape parameters, while a double star is an object which is wider than a single PSF and is fit by a linear combination of two stellar PSFs, each of which uses the current average shape parameters. An important parameter, STOGRAT, is defined as the critical ratio of χ^2 for a galaxy fit divided by χ^2 for a double star fit. If this ratio is observed to be less than the user-specified value of STOGRAT, DoPHOT classifies the object as a galaxy and the galaxy shape parameters are retained; otherwise the object is classified as a double star, and the PSF parameters for the two stellar objects are retained. Finally, in case 3, DoPHOT finds what it considers to be a ‘good’ star and the PSF parameters from this fit – using the newly derived shape parameters – are saved. After fitting and classifying each star in this way, the best-fitting PSF is subtracted from the cleaned array, the noise array is updated, and SHAPE moves on to the next star in the list.

At the end of its loop, SHAPE has a list of stars for which the PSF shape parameters were determined independently from their 7-parameter fits. A weighted average of these parameters results in a new set of average shape parameters that can be used in all subsequent 4-parameter fits. Note that SHAPE is designed to identify ‘good’ stars as isolated, high signal-to-noise images, and the stars that dominate the determination of the average shape parameters tend to include all stars that a user would pick interactively to construct the PSF. Consequently, the shape parameters vary only slightly after the first few threshold loops (see Table 1).

2.6 Improving the Fits

Armed with newly updated average shape parameters, DoPHOT again loops through the object list to a) confirm that each legitimate stellar object identified by ISEARCH still exists, b) compute 4-parameter fits for *all* stellar objects using the new average shape parameters, and c) compute an aperture magnitude for each object that can be used to calibrate the photometry. These tasks are represented by the lower horizontal line in Figure 1 and are controlled by the DoPHOT subroutine IMPROVE.

Threshold	N_{found}^a	σ_x^2	σ_{xy}	σ_y^2	N_{PSF}^b
3584	180	2.372	0.0077	2.817	103
1792	272	2.340	0.0064	2.810	169
896	493	2.340	0.0063	2.797	232
448	978	2.325	0.0061	2.788	373
224	1833	2.320	0.0064	2.787	661
112	2751	2.316	0.0065	2.788	694
56	3035	2.313	0.0063	2.788	693

a) N_{found} = the total number of objects found by DoPHOT at a given threshold.
b) N_{PSF} = the total number of stars used to estimate the shape parameters at a given threshold.

Table 1: Evolution of a DoPHOT reduction of a CCD frame.

As **IMPROVE** loops through the object list, it adds each object back to the cleaned array one-by-one and updates the noise array. Non-stellar objects are skipped at this stage because they have already been classified as objects that cannot be **IMPROVED**. For example, galaxies are, by definition, objects whose shape parameters differ significantly from the average shape parameters; a 4-parameter fit is not valid for them. Because **ISEARCH** assumed some knowledge of the average shape parameters in constructing the mask through which potential objects were identified, **IMPROVE** must repeat this step using the new average shape parameters (and, thus, a new mask) to confirm that the objects identified by **ISEARCH** are still present. This test usually confirms **ISEARCH**'s identifications except occasionally during the first few threshold passes when the average shape parameters are still poorly determined. Then, 4-parameter fits are performed on *all* legitimate stellar objects using the analytic PSF (equation 1 in our case). Even the 'good' stars used earlier by **SHAPE** to define the current average shape parameters are re-fit in this way. **IMPROVE** then calculates the total sky-subtracted intensity in a subraster centered on the star. The size of this subraster may differ from the size of the fit subraster, and is specified by the user. This last step provides an 'aperture correction' between the fitted magnitudes and the total brightness of the stellar images which is necessary to calibrate the data. The fit parameters, aperture magnitude, and formal fit errors are recorded for each star. The star is then subtracted from the cleaned array, the noise array is updated, and **IMPROVE** considers the next object in the list. When **IMPROVE** reaches the end of the object list, **DoPHOT** proceeds to **ISEARCH** in the next threshold loop, or the program terminates if this had been the last threshold loop. The final results include a file containing the cleaned array (which the user can immediately inspect), and another file with the identifications, fit parameters, aperture magnitudes and fit errors for every object identified by **DoPHOT**.

Figure 3 illustrates the appearance of the cleaned array at four stages of its reduction. The iterative approach that **DoPHOT** uses to identify progressively fainter stars and improve its estimate of the PSF is well illustrated by this figure.

2.7 Known Shortcomings and Advantages of DoPHOT

A recognized shortcoming of **DoPHOT** is its inability to fit more than two stars simultaneously. This problem is somewhat worse than it may at first seem because although **SHAPE** does an explicit two-star fit for doubles, the final 4-parameter fits performed in **IMPROVE** involve only one star at a time. A companion's presence is felt only through its contribution to the noise array. This limitation on

how the code handles multiple images was accepted in return for speed and simplicity. Nevertheless, although this method of handling merged stellar images is crude, it is apparent from the discussion below that DoPHOT still does quite well in crowded fields. Another known shortcoming of DoPHOT is the use of an analytic PSF. Again, this was done in the interests of speed, but this compromise does not appear to severely affect the photometry in moderately crowded fields. Still, the analytic PSF is never a perfect match to the true PSF, and each time a star is subtracted from the cleaned array, some residuals remain. The parameters associated with the noise array can be tuned to ensure that these residuals are not confused with faint stars. Thus, DoPHOT's use of a simple analytic PSF does *not significantly compromise the quality of its photometry*. Rather it primarily limits the program's ability to identify faint close companions of bright stars.

DoPHOT offers a number of definite advantages over most other photometry reduction programs. First, DoPHOT runs in an entirely automated manner, and the human time required to set-up and start reducing a frame is minimal. In addition, the bookkeeping that is inevitably associated with the identification and measurement of large numbers of objects on a two-dimensional picture is all handled by the code itself. Second, given a set of input parameters, a picture can be reduced with DoPHOT in a completely reproducible way. In contrast, programs that require a substantial amount of human intervention (either to generate the PSF, identify stars, or flag 'bad' stars, etc.) can be quite user-dependent¹. Thus, DoPHOT is particularly well-suited for luminosity function determinations or whenever frequent, very similar reduction passes are essential. Third, because of its numerous input parameters, DoPHOT is extremely flexible. This one program has been used to successfully reduce scanning CCD data, deep photometry in crowded fields in the LMC, and deep images of faint galaxies at high Galactic latitude fields. Having a large number of tuneable parameters may seem like a double-edged sword, but ongoing tests suggest that the photometry produced by DoPHOT does not change drastically even when the default values of its parameters are changed significantly. Finally, DoPHOT is fast. Recently, one of us (MM) obtained a series of 50 800×800 CCD images of the Carina dwarf galaxy to search for faint, short-period variables using the CTIO 4m telescope. Using DoPHOT, one user was able to measure every one of these frames and a total of about 150000 stellar images in less than four days. All the jobs were run in batch mode, and at the completion of the reduction of one frame, the next was automatically started.

3 Testing DoPHOT

Testing a photometry program such as DoPHOT is difficult because of the endless variety of telescope/detector/object combinations that are possible. Nevertheless, we have applied DoPHOT to a wide range of reduction problems, and we can describe qualitatively how the program has performed. A quantitative assessment of the program is far more difficult because, in general, the 'true' answers are not known. In practice, the most meaningful quantitative tests involve comparisons of photometric results derived from repeated observations of a given field. In this section we describe some of the tests we have subjected DoPHOT to in order to assess the range of applicability of the code, and provide a quantitative estimate of its repeatability.

3.1 The ESO Test Images

We have reduced 12 of the 15 test images provided by ESO for this workshop with DoPHOT. The photographic data of the Vela supernova remnant and the Coma dwarf galaxy CCD image were not suitable for analysis with DoPHOT because of complex non-linearity and background problems. A summary of the reductions is provided in Table 2. All calculations were performed with a μ VAX 3

¹These user-dependent tasks are often referred to as the 'art' of doing photometry. DoPHOT's repeatability makes it more like a wrench than a paintbrush.

Object	Filter	CPU Time (hh:mm)	# Detected Objects
Fornax	V	00:22	1501
Fornax	B	00:26	1138
47 Tuc Center	V	03:55	5811
47 Tuc Center	B	03:20	5209
47 Tuc Outer	V	00:15	695
47 Tuc Outer	B	00:14	634
Galaxy Cluster	r	00:25	231
Galaxy Cluster	r	00:53	470
NGC 3210	V	00:35	2310
NGC 3210	V	00:30	1802
SGP	B _J	00:02	1211
SGP	R	00:02	490

Table 2: Reduction of ESO test frames.

which runs DoPHOT about 3.8 times faster than a VAX 11/750. Each frame required about 10 minutes of human setup time, but the actual DoPHOT reductions were completely automatic. The tabulated results of our analyses of these test frames are available on a VAX Backup tape at ESO headquarters.

Fornax — DoPHOT was able to reduce these frames in a straightforward manner. The resulting color-magnitude diagram (CMD) contains 565 stars and is shown in Figure 4. The main features visible in this figure agree qualitatively very well with the results of Buonanno [1].

Central Region of 47 Tuc — These very crowded pictures were the most demanding of the ESO images to reduce with DoPHOT. Nevertheless, with very little human time expended, the program was able to produce a CMD that agrees qualitatively very well with the results presented by Ortolani [3] using the same data but different reduction programs. A total of 2403 stars were matched in the B and V frames to construct the CMD.

Outer field of 47 Tuc — These frames were easily and quickly reduced by DoPHOT. The color distributions along three 0.5-mag wide cuts in V are shown in Figure 5. The number of main sequence stars detected by DoPHOT in these cuts (33–35) is essentially identical to the number found by Ortolani [3] in his analysis of the same data.

The galaxy cluster 0637-53 — Because their radial profiles differ so much from that of single stars, the outer regions of the two bright elliptical galaxies in these frames were not fit properly by DoPHOT. Consequently, the program identified and measured a number spurious objects in the residuals of these galaxies in the cleaned picture. DoPHOT was able to classify 80 stars and 73 galaxies among the brightest objects identified on the deeper frame. However, the faintest 167 objects could not be classified using DoPHOT's current image classification criteria. The reduction of these frames took the most human time to reduce because a number of parameters (e.g., the fit subraster size, STOGRAF, and the detection limits) were adjusted to optimize DoPHOT for the specific difficulties posed by the data.

NGC 3201 — This test of linearity based on reductions of 1 and 10 minute exposures of the same

field was complicated by the undersampled images and relatively low dynamic range in both frames. Nevertheless, DoPHOT was able to reduce these frames easily, and a plot of the magnitude differences between common stars is shown in Figure 6. There is a significant slope of 0.025 mag/mag evident in the figure, but the standard deviation about the best-fitting line averages about 0.02 mag for the five brightest 0.5-mag bins.

Deep SGP fields — As seen in Table 2, DoPHOT was able to detect and measure over 1200 images on the deep B_J images of the SGP, but considerably fewer on the R frame. A CMD constructed from these results agrees qualitatively very well with the one shown by Tyson [5] for the same field. However, as in the case of the images of the galaxy cluster 0637–53, the version of DoPHOT used here was unable to classify the faintest objects.

3.2 Repeatability Tests

Low Galactic latitude fields — Ten square degrees of a relatively clear area within 1° of the Galactic plane were scanned seven times using the Las Campanas Observatory (LCO) 1m telescope and an RCA CCD by J. Caldwell and PS. The effective integration time of these scans was about 17 sec. Based on repeat measurements, they have found that a single observation is accurate to 0.015 mag for $9 < I < 13$, rising to 0.04 mag by $I = 14$. The PSF used to reduce these data was of a different form than equation 1, and was allowed to vary smoothly to account for geometric distortions in the optical system, as well as seeing variations during the scan.

The globular cluster M5 — We have access to a large set of high-quality CCD images of the rich globular cluster M5 which includes a number of repeat observations of some fields in and around this object. These data were obtained with a number of different telescopes and provide a good test of a photometry program's internal repeatability. One test involves four RCA CCD BV images obtained on two different nights with the KPNO 0.9m telescope. Although the images are nearly critically sampled (FWHM ~ 2.2 pix), the DoPHOT magnitudes and colors agree quite well. Specifically, for $V \lesssim 14.5$ the standard deviation of the difference in the V magnitudes and (B–V) colors for the 20 brightest stars are 0.014 mag and 0.009 mag, respectively². Note that the (B–V) comparisons involve *four* frames, and so the implied precision of a single observation is about 0.005 mag. The larger scatter for the V photometry could possibly indicate some small intrinsic variations in the luminous giants in M5. P. Harding and I. Thompson have recently obtained TI CCD images of M5 with the LCO 1m and 2.5m telescopes. The data from the 2.5m are well-sampled (stellar FWHM ~ 4 –5 pix) and the analytic PSF described by equation 1 does not fit the wings of the stellar images that well. Nevertheless, they find that the repeatability of the DoPHOT magnitudes is quite good ($\lesssim 1.5\%$) for the brighter stars³.

Carina — The Carina frames mentioned at the end of §II provide an excellent test of DoPHOT's ability to reproduce its results in a relatively uncrowded field. Two sets of about 25 500 sec TI CCD frames were obtained with the CTIO 4m telescope on consecutive nights over a total of 8 hours. One of these sets of data consist of 16 V frames taken over 3.5 hours. The stellar profiles are well-sampled, but their widths varied over the course of the observations from 2.9 to 4.2 pix FWHM. Nevertheless, for 42 stars with $18.5 < V < 20.7$, and measured on all 16 frames, the average of the standard deviations of the individual mean magnitudes is 0.014 mag. This becomes 0.012 mag if three stars with observed standard deviations that are 2.5σ away from the mean are excluded. The mean formal error in both cases is 0.009 mag.

²As an aside, one of us (MM) has reduced these frames using DAOPHOT and found that the night-to-night agreement in the V magnitudes for the same stars is 0.024 mag.

³For these data, DAOPHOT appears to be doing as well.

4 Conclusion

In this paper, we have described in some detail how the DoPHOT photometry program operates, emphasizing the code's versatility, automatic operation, and the basic assumptions that are built into the reduction algorithm. The main purpose of this contribution is to describe a *method* of doing digital photometry, and how this method is implemented within the DoPHOT code. Although we have no general plan for distribution of the code itself, this is not ruled out in the future if there is sufficient outside interest and local support for this to be practical.

DoPHOT is currently being used to help address a number of scientific problems. These include a) the study of stellar populations in nearby galaxies, b) identification of faint main sequence variable stars in dwarf galaxies, c) construction of deep Gunn system CMDs and luminosity functions in Galactic globular clusters, d) determinations of the abundances of Magellanic Cloud clusters using Washington CCD photometry, e) measurements of the photometric properties of Cepheid variables in nearby galaxies to determine their distances and in Magellanic Cloud clusters in order to constrain Cepheid evolutionary models, f) identification of high latitude K dwarfs to use to study the gravitational potential of the Galactic disk, g) searches for low-latitude Cepheids to be used to measure the Galactic rotation curve, and h) surveys of faint quasars to improve the faint end of the QSO luminosity function. These projects are based on CCD observations obtained with a number of different telescopes; some are based on CCD scan data. Practical experience and tests using these data have proven that DoPHOT is a fast, flexible, and accurate tool with which to address all of these issues and the specific reduction problems they entail.

Future plans for the code include possible improvements in the form of the adopted PSF – perhaps even the use of an automatically generated empirical PSF. The main difficulty with expending a considerable effort in such improvements is that, in our view, it is not clear that they are really justified given the limited gains that would result from being able to perform fits to a few additional faint, close stellar companions. In addition, in collaboration with S. Shectman, we have begun investigating the possibility of reducing scanning CCD data *in real time*. This would be especially helpful for projects involving searches for transient objects (variable stars, minor planets, etc.), and to remove the huge reduction burden from the observer who obtains large-scale CCD scans.

Acknowledgements: We thank John Caldwell for making Figure 1 and for his efforts in reducing some of the scanning data that are referred to in this paper. It is a pleasure to thank S. Anderson, K. Cook, W. Freedman, P. Harding, and S. Hawley for their help in sharing with us their practical experiences with DoPHOT. Thanks also to S. Drescher for her help in constructing Figure 3. DoPHOT was developed with support from grant AST 83-18504 from the National Science Foundation of the United States, and part of the computing reported in this paper was possible with the support of NSF grant AST 87-13889 to W. Freedman.

References

- [1] Buonanno, R. Corsi, C. E., Fusi Pecci, F., Hardy, E., Zinn, R. : 1985, *Astron. Astrophys.*, **152**, 349.
- [2] Lupton, R. H., and Gunn, J. E. : 1986, *Astron. J.*, **91**, 317.
- [3] Ortolani, S., Murtagh, F. : 1989, this volume.
- [4] Press, W. H., Flannery, B. P., Teukolsky, S. A., and Vetterling, W. T. : 1986, *Numerical Recipes*, (Cambridge, Cambridge University Press).

- [5] Tyson, J. A. : 1988, *Astron. J.*, **96**, 1.

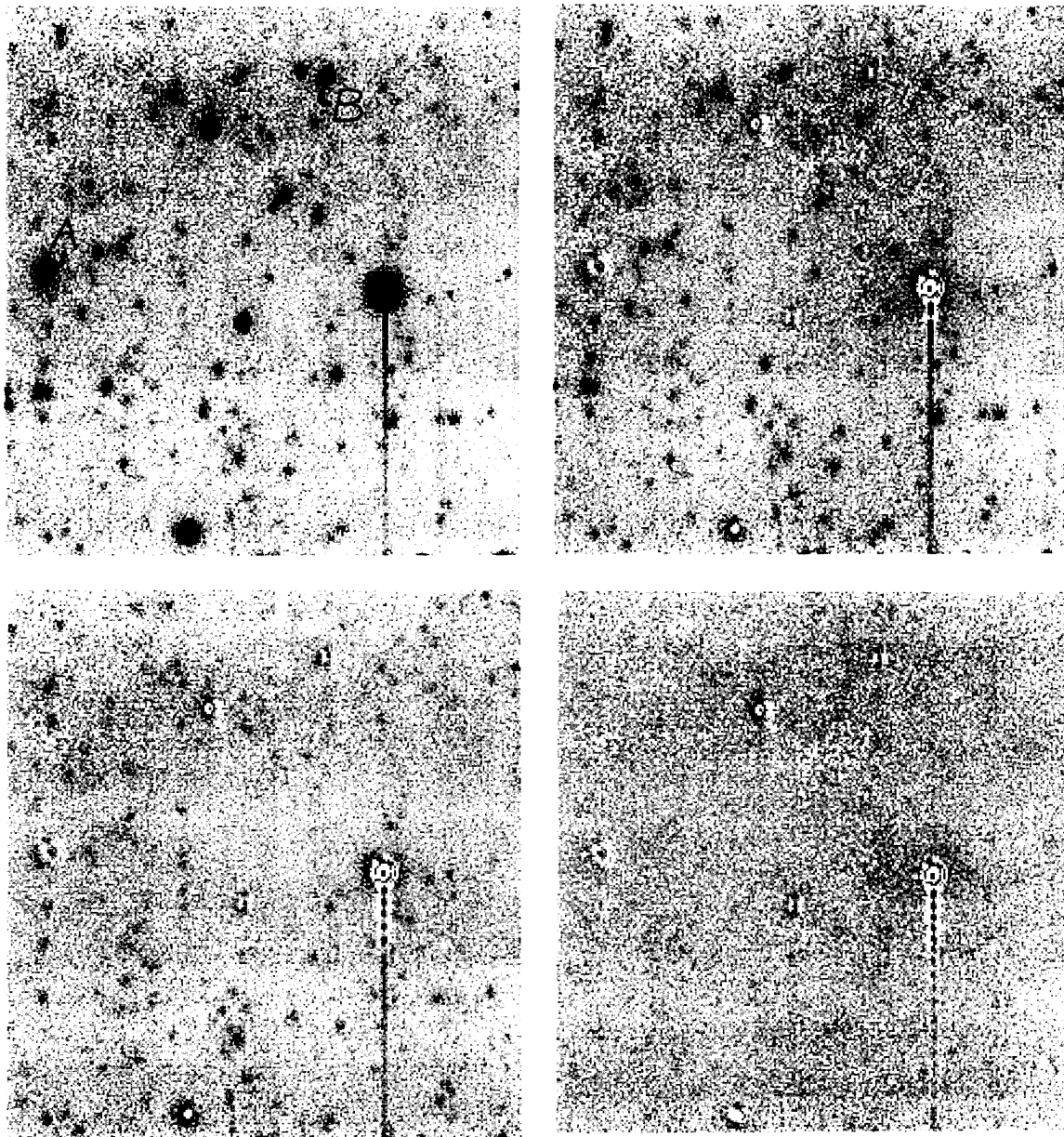


Figure 3: Four snapshots of the central region of a cleaned array during a reduction run using DoPHOT. The upper left figure is the original image; the upper right is after the second threshold loop; the lower left is after the fifth threshold loop; and the lower right is the cleaned array after DoPHOT completed its reduction. Note how progressively fainter stars are identified and then removed from the picture. Object A was classified as a galaxy by DoPHOT, and it is apparent that its profile is skewed compared to the stellar profiles. Also, one can see that near the final threshold, DoPHOT found and fit the residuals of object A with faint stars. This is common around resolved galaxies because the stellar PSF is (understandably) a poor fit for such objects. Object B is a pair of stars as is apparent after the brighter companion is identified and subtracted. Note, however, that the fainter star was also ultimately found and fit by DoPHOT.

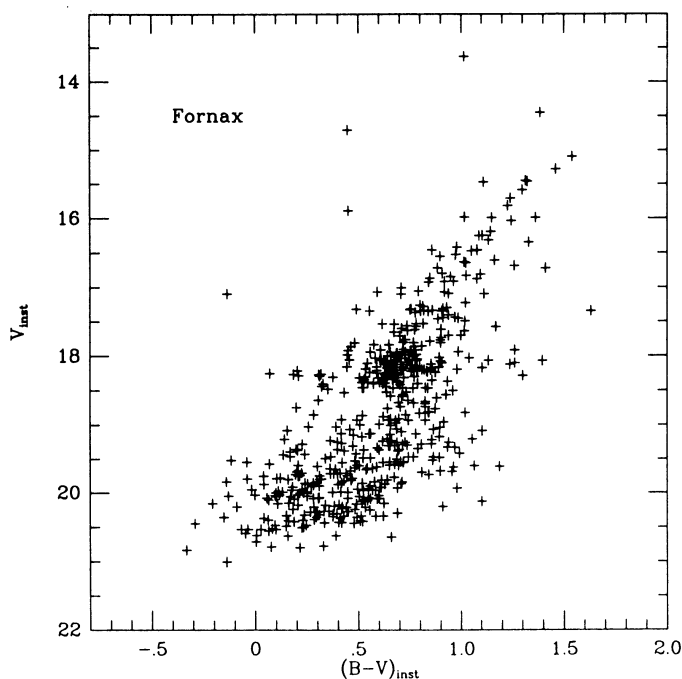


Figure 4: A V-(B-V) CMD of the Fornax dwarf galaxy based on a pair of ESO test images distributed for this workshop and reduced with DoPHOT.

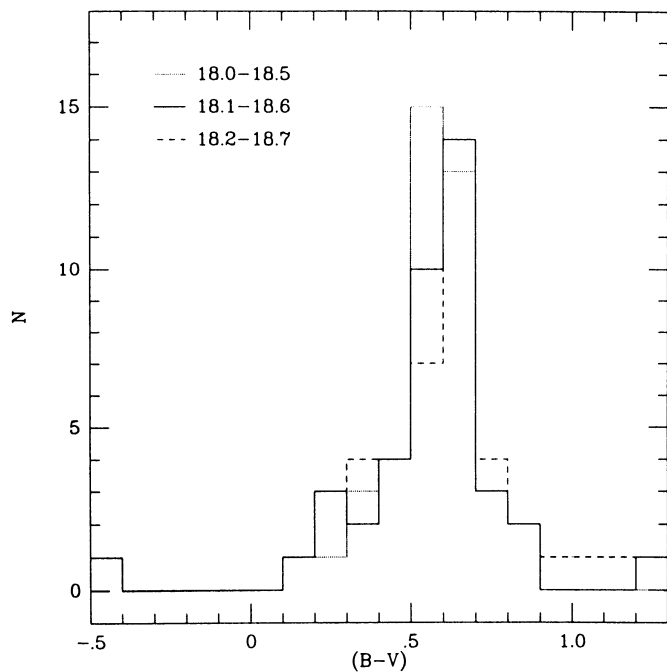


Figure 5: The color distributions along three 0.5-mag cuts across the CMD of an outer field of 47 Tuc and based on the reduction of a pair of ESO test images with DoPHOT.

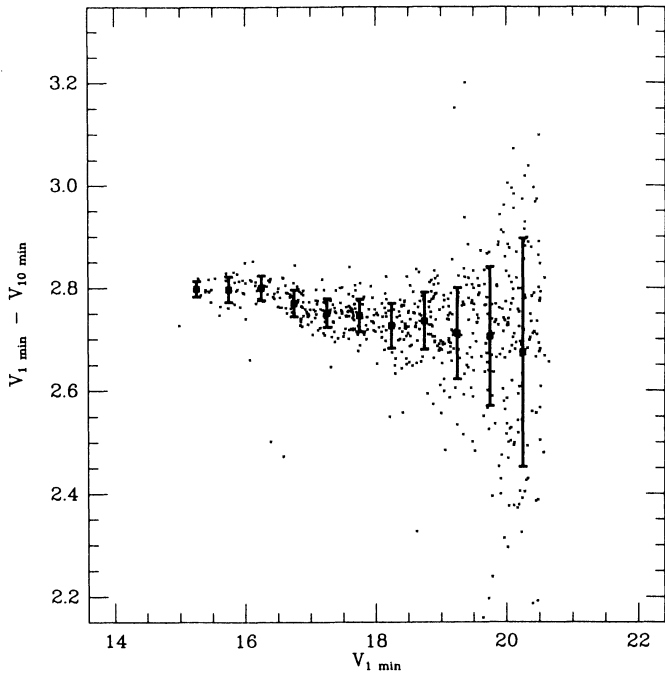


Figure 6: A plot of the difference in instrumental magnitudes between the 1 and 10 minute ESO test images of the globular cluster NGC 3201. The small kink at $V_x x$ corresponds to the point where the central intensities of the stars reach the digital saturation limit of the deeper frame.